
CLIP meets Model Zoo Experts: Pseudo-Supervision for Visual Enhancement

Anonymous Author(s)

Affiliation

Address

email

Abstract

1 Contrastive language image pretraining (CLIP) is a standard method for training
2 vision-language models. While CLIP is scalable, promptable, and robust to distri-
3 bution shifts on image classification tasks, it lacks object localization capabilities.
4 This paper studies the following question: *Can we augment CLIP training with*
5 *task-specific vision models from model zoos to improve its visual representations?*
6 Towards this end, we leverage open-source task-specific vision models to gener-
7 ate pseudo-labels for an uncurated web-scale image-text dataset. Subsequently,
8 we train CLIP models on these pseudo-labels in addition to the contrastive train-
9 ing on image and text pairs. This simple setup shows substantial improvements
10 of up to 16.3% across different vision tasks, including segmentation, detection,
11 depth estimation, and surface normal estimation. Importantly, these enhancements
12 are achieved without compromising CLIP’s existing capabilities, including its
13 proficiency in promptable zero-shot classification.

14 1 Introduction

15 Foundation Models (FMs) are revolutionizing different domains of artificial intelligence and machine
16 learning, including computer vision [31, 14, 17] and natural language processing [7, 2, 41]. FMs
17 can be trained on web crawled data without relying on crowd or expert annotations, and yet they
18 demonstrate strong generalization capabilities [15, 36].

19 CLIP, one of the most prominent methods for FM training in vision, uses contrastive learning to align
20 image and text representations [31, 15]. In addition to robustness to data distribution shifts, CLIP
21 offers impressive zero-shot and cross-modal retrieval capabilities on unseen datasets. Nevertheless,
22 computer vision encompasses a broad range of tasks that require the ability to comprehend spatial
23 relationships, semantic content, object localization, and 3D structures. In spite of CLIP’s impressive
24 zero-shot open-vocabulary classification accuracy, it exhibits poor localization capabilities and often
25 struggles in associating text with objects in an image [40, 12, 32]. Consequently, in practice, many
26 vision tasks (e.g., detection and segmentation), rely on CLIP through fine-tuning the entire model to
27 compensate for these localization deficiencies.

28 In this work, we seek to answer the following question: *Can we augment pretrained CLIP models with*
29 *task-specific vision models from model zoos to improve its visual representations?* That is, we seek to
30 (1) use open-source task-specific vision models to generate *hard* pseudo-labels on a web-scale noisy
31 image-text dataset and, (2) train CLIP on image-text pairs along with pseudo-labels with multiple
32 objectives. An overview of our approach, which we call **CLIP Training with eXperts (CLIPTeX)**, is
33 shown in Fig. 1. We show that CLIPTeX enhances the visual representations of CLIP and yields up
34 to 16.3% enhancement in probing accuracy across a diverse set of vision tasks and datasets while
35 preserving the existing capabilities of CLIP models, including prompting for zero-shot classification.

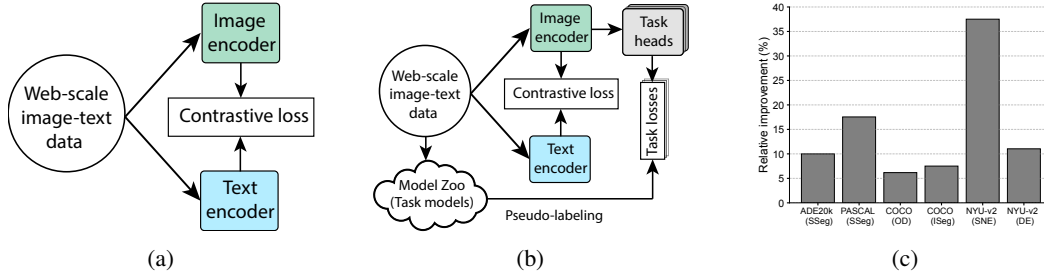


Figure 1: **Training CLIP with pseudo-labels improves its visual representations.** (a) shows the standard CLIP training. (b) shows CLIPTeX that trains CLIP with pseudo-labels from experts. Note that the main purpose of task heads is to improve CLIP’s image encoder with expert knowledge, and the heads can be discarded after training. (c) shows the relative improvement that CLIPTeX obtains over CLIP-FT. Here, SSeg, OD, ISeg, SNE, and DE refer to semantic segmentation, object detection, instance segmentation, surface normal estimation, and depth estimation respectively.

36 2 CLIPTeX

37 **Model** CLIPTeX extends CLIP with pseudo-supervision from publicly available task experts spe-
 38 cializing in localization, depth, and surface normal estimation. Our approach enhances CLIP’s
 39 representations *without any labeled data collection* (Fig. 1). Similar to CLIP, CLIPTeX uses two
 40 encoders: (1) an image encoder that takes an RGB image and produces an image embedding and (2)
 41 a text encoder that takes the text caption and produces a text embedding.

42 In addition to contrastive training, we would like to train CLIPTeX using pseudo-labels. Towards
 43 that end, we incorporate task-specific heads that take the output of image encoder as input and
 44 generate predictions for the respective task (see Fig. 1b). Previous work have shown that multi-scale
 45 representations provides significant benefit in tasks requiring localization and fine-grained visual
 46 understanding [49, 22]. However, some image encoders (e.g., ViT) do not inherently possess these
 47 capabilities. To ensure CLIPTeX can learn better visual representations independent of the image
 48 backbone, we include a single shared multi-scale module [49] between image encoder and task-
 49 specific heads. We feed the output of the image encoder through a multi-scale module [49], which in
 50 turn feeds into the lightweight task-specific classification or regression heads. In our implementation,
 51 we use independent point-wise convolution as the head for each task. As the task’s head output
 52 dimensions should match input dimensions in dense prediction tasks, we perform nearest neighbour
 53 interpolation on head’s output if necessary.

54 **Training objective** To train CLIPTeX with pseudo-supervision on n tasks, we generate *hard* pseudo-
 55 labels offline using publicly available task-specific experts on an uncurated web-scale dataset. We
 56 then train CLIPTeX with a weighted sum of contrastive loss and task-specific losses: $\mathcal{L} = \lambda_{\text{clip}} \cdot$
 57 $\mathcal{L}_{\text{clip}} + \sum_{t=1}^n \lambda_{\text{task}}^t \cdot \mathcal{L}_{\text{task}}^t$ where $\mathcal{L}_{\text{task}}^t$ is the loss of the t -th task and $\mathcal{L}_{\text{clip}}$ is the contrastive loss. Here,
 58 λ_{task}^t and λ_{clip} are the loss coefficients of t -th task and the standard CLIP loss, respectively.

59 3 Experimental Setup

60 Probing, a standard method to study the representations learnt by neural networks [14, 31], is used to
 61 investigate whether pseudo-supervision in CLIPTeX can improve CLIP’s image backbone.

62 **Task-specific experts** We train CLIPTeX with hard pseudo-labels generated from following experts:
 63 (1) *Semantic segmentation*. We use Mask-RCNN [13] with ViT backbone [8], trained on the COCO
 64 [21] with RangeAugment [27], to produce pseudo-labels for segmentation. (2) *Monocular depth*
 65 *estimation*: We use DPT [33], trained on MIX-6 dataset [33], to generate monocular depth map
 66 pseudo-labels. (3) *Surface normal estimation*: We use *NLL-AngMF* [1] as our surface normal expert,
 67 which is trained on ScanNet dataset [6].

68 **Baselines** We compare with following baselines: (1) *CLIP*. We use CLIP model [26] pretrained
 69 on 1.2 billion images with a variable resolution and batch sampler whose base input image’s spatial

Table 1: **Probing results for different vision tasks.** Pseudo-labeling in CLIPTeX significantly improves the visual representations in the image encoder of CLIP.

Model	Segmentation(\uparrow)		Detection(\uparrow)		Depth(\downarrow)		Surface normal (\uparrow)		Classification(\uparrow)
	Linear	PSPNet	Mask-RCNN	SSD	Linear	PSPNet	Linear	PSPNet	Linear
ViT-B/16									
CLIP	18.66	45.53	15.20	5.33	0.235	0.168	28.49	47.29	80.24
CLIP-FT	62.47	78.22	27.21	16.46	0.215	0.139	29.06	47.91	79.94
CLIPTeX (Ours)	73.43	80.71	28.89	17.50	0.159	0.128	39.96	50.80	79.64
ViT-H/16									
CLIP	56.18	75.37	26.65	11.07	0.212	0.132	29.09	49.78	84.85
CLIP-FT	62.95	82.94	33.93	20.24	0.213	0.125	29.21	50.48	84.1
CLIPTeX (Ours)	79.30	84.31	34.50	21.55	0.138	0.117	43.22	53.89	83.2
ResNet-50									
CLIP	46.96	70.92	29.49	20.32	0.212	0.147	33.67	47.28	78.35
CLIP-FT	34.78	74.17	38.13	30.28	0.239	0.155	28.72	48.66	78.92
CLIPTeX (Ours)	40.31	75.58	38.23	28.62	0.220	0.150	31.56	49.44	78.95

70 resolution is 224×224 . (2) *CLIP-FT*. Many dense prediction tasks (e.g., segmentation) benefit
71 from using high-resolution input images. To have a fairer baseline trained on the same resolution
72 as CLIPTeX, we finetune CLIP with contrastive loss on CC3M. The training is done with variable
73 resolution using a batch sampler whose base input image resolution is 512×512 . Any improvements
74 over this baseline signify a pure transfer of knowledge from pseudo-supervision.

75 To show the generality of CLIPTeX, we experiment with three image encoder backbones: ViT-B/16,
76 ViT-H/16, and ResNet-50. Also note that we finetune CLIPTeX on CC3M’s image and text pairs
77 along with pseudo-labels using the same settings as CLIP-FT. We use cross-entropy loss to train on
78 segmentation pseudo-labels, and L1 loss to train on depth and surface normal pseudo-labels.

79 **Evaluation downstream tasks and datasets** We evaluate the models using classifier and regressor
80 probes on the following tasks: (1) *Semantic segmentation*. We use PASCAL VOC [9] with 20
81 classes. We report mean intersection over union (mIoU) on the validation set. (2) *Object detection*
82 *and instance segmentation*. The models are evaluated on COCO dataset for detection and instance
83 segmentation. Importantly, during training with pseudo-labels, we do not use the bounding boxes.
84 Instead, the instance masks are converted to semantic segmentation pseudo-labels. This allows us
85 to evaluate baselines on both instance segmentation and object detection, which are considered to
86 be more challenging tasks than semantic segmentation. Following standard convention, we evaluate
87 the accuracy on COCO’s validation set in terms of mean average precision (mAP). (3) *Monocular*
88 *depth estimation*. We use NYU-V2 [29] dataset as our depth estimation benchmark. Note that DPT,
89 the expert used for depth pseudo-supervision, is trained on a different dataset, i.e., ScanNet. We use
90 absolute relative error as a metric for evaluation on the validation set. (4) *Surface normal estimation*.
91 We use NYU-V2 for surface normal estimation. We train on the training set used by Bae et al. [1]
92 and Qi et al. [30], and evaluate on the official test set of NYU-V2. Following [1], we use $a < 30$
93 as the metric for evaluation. (5) *Image classification*. We evaluate on ImageNet 1K [35] classification
94 dataset and top-1 accuracy on the validation set is reported as the evaluation metric.

95 **Classifier and regressor probes for evaluation** To study the visual representations of different
96 *frozen* pre-trained models, our experiments involve both classification and regression tasks across
97 different datasets. For dense prediction tasks, such as semantic segmentation, depth, and surface
98 normal estimation we probe frozen image encoders with two types of probes: (1) Linear which is
99 a point-wise convolutional layer. (2) PSPNet [49], a standard non-linear head for dense prediction
100 tasks. For image classification a fully-connected layer is used as the linear probe. For object detection
101 and instance segmentation, Mask R-CNN [13] and SSD heads are used. Additional probing results
102 with different heads (e.g. DeepLabV3) and tasks (e.g. ADE20k) are included in Appendix C.

103 4 Results

104 **Pseudo-supervision improves visual representations** Probing results for all tasks are given in
105 Table 1. In semantic segmentation, CLIPTeX shows consistent improvements over the baselines.
106 Particularly noteworthy is the linear probing accuracy of CLIPTeX with ViT-B/16 and ViT-H/16
107 backbones on the PASCAL VOC dataset, which is about 10% and 16.3% better than CLIP-FT.

Table 2: **CLIP’s zero-shot knowledge is preserved after training with experts.** (a) report zero-shot top-1 accuracy for ImageNet-1k dataset and (b) reports recall@1/5/10 for Flickr-30k dataset.

(a) 0-shot classification on ImageNet.

Model	0-shot Top-1
CLIP-FT	68.76
CLIPTeX (Ours)	68.25

(b) 0-shot retrieval on Flickr-30k.

Model	Text Retrieval			Image Retrieval		
	R@1	R@5	R@10	R@1	R@5	R@10
CLIP-FT	85.90	96.70	98.60	71.66	91.00	94.94
CLIPTeX (Ours)	86.00	96.90	98.70	71.40	90.86	95.16

Table 3: **Role of pseudo-labels from each experts in CLIPTeX training.**

Row #	Expert			Segmentation (\uparrow)		Detection (\uparrow)		Depth (\downarrow)		Surface Normal (\uparrow)	
	Segmentation	Depth	Surface Normal	Linear	PSPNet	Mask R-CNN	SSD	Linear	PSPNet	Linear	PSPNet
R1	\times	\times	\times	62.47	78.22	27.21	16.46	0.215	0.139	29.06	47.91
R2	\checkmark	\times	\times	72.21	81.39	28.54	17.58	0.203	0.136	34.86	48.62
R3	\times	\checkmark	\times	64.50	81.16	27.75	16.70	0.170	0.131	35.21	49.51
R4	\times	\times	\checkmark	63.28	81.48	27.69	16.81	0.193	0.134	37.42	50.71
R5	\checkmark	\checkmark	\times	73.96	81.49	28.83	17.57	0.162	0.130	37.05	49.69
R6	\checkmark	\times	\checkmark	72.67	81.30	28.83	17.75	0.188	0.132	38.65	50.48
R7	\times	\checkmark	\checkmark	64.20	81.17	27.90	17.00	0.165	0.129	39.59	51.01
R8	\checkmark	\checkmark	\checkmark	73.43	80.71	28.89	17.50	0.159	0.128	39.96	50.49

108 For object detection with ViT-B/16 as the frozen backbone and Mask-RCNN as the probing head,
 109 CLIPTeX delivers 13.69% and 1.68% better bounding box mAP over CLIP and CLIP-FT respectively.
 110 We observe similar gains when CLIPTeX is probed with SSD.

111 For depth estimation, CLIPTeX obtains lower error rate, while for surface normal estimation, CLIPTeX
 112 obtains higher value of $a < 30$ compared to CLIP and CLIP-FT baselines. These results indicate
 113 a positive transfer of distance and surface orientation knowledge to CLIPTeX’s image backbone,
 114 contributing to the better performance.

115 Unlike other dense prediction tasks, CLIP achieves similar or slightly better accuracy compared to
 116 CLIP-FT and CLIPTeX. This outcome can be attributed to the characteristics of image classification
 117 tasks as it primarily focuses on recognizing objects without requiring detailed information about
 118 spatial relationships or 3D structure of the scene.

119 **Zero-shot capabilities are preserved in CLIPTeX** One of the important and powerful characteris-
 120 tics of CLIP is *prompting*, which enables zero-shot transfer to new datasets. Pseudo-supervision with
 121 experts can potentially lead to catastrophic forgetting of previously learned knowledge, which may in
 122 turn affect model’s zero-shot generalization capabilities. Table 2 compares the zero-shot capabilities
 123 of CLIP-FT and CLIPTeX in classification on ImageNet-1k [35] and retrieval on Flickr-30k [45]
 124 tasks respectively. CLIPTeX’s zero-shot performance is on par with that of CLIP-FT, indicating that
 125 enhanced representations do not result in catastrophic forgetting.

126 **Ablation on the importance of pseudo-labels in CLIPTeX.** Incorporating pseudo-supervision
 127 from task-specific experts, even from a single expert during training, results in substantial im-
 128 provements in performance. These improvements are observed when evaluating models on various
 129 downstream tasks with different probes (see R1 vs. rest; Table 3). Overall, our findings indicate
 130 that incorporating knowledge from all experts contributes to learning better visual representations.
 131 Therefore, we use all experts for pseudo-supervision while training CLIPTeX.

132 5 Conclusion

133 As the field of machine learning research embraces openness, a growing number of specialized
 134 expert models become publicly available. Our study showcased the potential of leveraging these
 135 publicly available expert models to enhance CLIP’s visual representations, all without the necessity
 136 of collecting task-specific data. Our experiments revealed that CLIPTeX yields improvements across
 137 a wide range of tasks, highlighting its versatility and effectiveness.

References

- [1] G. Bae, I. Budvytis, and R. Cipolla. Estimating and exploiting the aleatoric uncertainty in surface normal estimation. *CoRR*, abs/2109.09881, 2021. URL <https://arxiv.org/abs/2109.09881>.
- [2] T. Brown, B. Mann, N. Ryder, M. Subbiah, J. D. Kaplan, P. Dhariwal, A. Neelakantan, P. Shyam, G. Sastry, A. Askell, et al. Language models are few-shot learners. *Advances in neural information processing systems*, 33:1877–1901, 2020.
- [3] M. Caron, H. Touvron, I. Misra, H. Jégou, J. Mairal, P. Bojanowski, and A. Joulin. Emerging properties in self-supervised vision transformers. In *Proceedings of the IEEE/CVF international conference on computer vision*, pages 9650–9660, 2021.
- [4] R. Caruana. Multitask learning. *Machine learning*, 28:41–75, 1997.
- [5] T. Chen, S. Saxena, L. Li, T.-Y. Lin, D. J. Fleet, and G. Hinton. A unified sequence interface for vision tasks, 2022.
- [6] A. Dai, A. X. Chang, M. Savva, M. Halber, T. A. Funkhouser, and M. Nießner. Scannet: Richly-annotated 3d reconstructions of indoor scenes. *CoRR*, abs/1702.04405, 2017. URL <http://arxiv.org/abs/1702.04405>.
- [7] J. Devlin, M.-W. Chang, K. Lee, and K. Toutanova. Bert: Pre-training of deep bidirectional transformers for language understanding. *arXiv preprint arXiv:1810.04805*, 2018.
- [8] A. Dosovitskiy, L. Beyer, A. Kolesnikov, D. Weissenborn, X. Zhai, T. Unterthiner, M. Dehghani, M. Minderer, G. Heigold, S. Gelly, J. Uszkoreit, and N. Houlsby. An image is worth 16x16 words: Transformers for image recognition at scale. *CoRR*, abs/2010.11929, 2020. URL <https://arxiv.org/abs/2010.11929>.
- [9] M. Everingham, L. V. Gool, C. K. I. Williams, J. M. Winn, and A. Zisserman. The pascal visual object classes (voc) challenge. *International Journal of Computer Vision*, 88:303–338, 2010. URL <https://api.semanticscholar.org/CorpusID:4246903>.
- [10] S. Y. Gadre, G. Ilharco, A. Fang, J. Hayase, G. Smyrnis, T. Nguyen, R. Marten, M. Wortsman, D. Ghosh, J. Zhang, et al. Datacomp: In search of the next generation of multimodal datasets. *arXiv preprint arXiv:2304.14108*, 2023.
- [11] G. Ghiasi, B. Zoph, E. D. Cubuk, Q. V. Le, and T.-Y. Lin. Multi-task self-training for learning general representations, 2021.
- [12] G. Ghiasi, X. Gu, Y. Cui, and T.-Y. Lin. Scaling open-vocabulary image segmentation with image-level labels, 2022.
- [13] K. He, G. Gkioxari, P. Dollár, and R. B. Girshick. Mask R-CNN. *CoRR*, abs/1703.06870, 2017. URL <http://arxiv.org/abs/1703.06870>.
- [14] K. He, X. Chen, S. Xie, Y. Li, P. Dollár, and R. Girshick. Masked autoencoders are scalable vision learners. In *Proceedings of the IEEE/CVF conference on computer vision and pattern recognition*, pages 16000–16009, 2022.
- [15] C. Jia, Y. Yang, Y. Xia, Y.-T. Chen, Z. Parekh, H. Pham, Q. Le, Y.-H. Sung, Z. Li, and T. Duerig. Scaling up visual and vision-language representation learning with noisy text supervision. In *International conference on machine learning*, pages 4904–4916. PMLR, 2021.
- [16] A. Kirillov, E. Mintun, N. Ravi, H. Mao, C. Rolland, L. Gustafson, T. Xiao, S. Whitehead, A. C. Berg, W.-Y. Lo, P. Dollár, and R. Girshick. Segment anything, 2023.
- [17] A. Kirillov, E. Mintun, N. Ravi, H. Mao, C. Rolland, L. Gustafson, T. Xiao, S. Whitehead, A. C. Berg, W.-Y. Lo, et al. Segment anything. *arXiv preprint arXiv:2304.02643*, 2023.
- [18] K. Lasinger, R. Ranftl, K. Schindler, and V. Koltun. Towards robust monocular depth estimation: Mixing datasets for zero-shot cross-dataset transfer. *CoRR*, abs/1907.01341, 2019. URL <http://arxiv.org/abs/1907.01341>.

- 185 [19] D.-H. Lee et al. Pseudo-label: The simple and efficient semi-supervised learning method for
186 deep neural networks. In *Workshop on challenges in representation learning, ICML*, volume 3,
187 page 896. Atlanta, 2013.
- 188 [20] L. H. Li, P. Zhang, H. Zhang, J. Yang, C. Li, Y. Zhong, L. Wang, L. Yuan, L. Zhang, J.-N. Hwang,
189 et al. Grounded language-image pre-training. In *Proceedings of the IEEE/CVF Conference on*
190 *Computer Vision and Pattern Recognition*, pages 10965–10975, 2022.
- 191 [21] T. Lin, M. Maire, S. J. Belongie, L. D. Bourdev, R. B. Girshick, J. Hays, P. Perona, D. Ramanan,
192 P. Dollár, and C. L. Zitnick. Microsoft COCO: common objects in context. *CoRR*, abs/1405.0312,
193 2014. URL <http://arxiv.org/abs/1405.0312>.
- 194 [22] T.-Y. Lin, P. Dollár, R. Girshick, K. He, B. Hariharan, and S. Belongie. Feature pyramid
195 networks for object detection, 2017.
- 196 [23] S. Liu, E. Johns, and A. J. Davison. End-to-end multi-task learning with attention, 2019.
- 197 [24] S. Liu, L. Fan, E. Johns, Z. Yu, C. Xiao, and A. Anandkumar. Prism: A vision-language
198 model with an ensemble of experts, 2023.
- 199 [25] J. Lu, C. Clark, R. Zellers, R. Mottaghi, and A. Kembhavi. Unified-io: A unified model for
200 vision, language, and multi-modal tasks, 2022.
- 201 [26] S. Mehta, S. Naderiparizi, F. Faghri, M. Horton, L. Chen, A. Farhadi, O. Tuzel, and M. Raste-
202 gari. Rangeaugment: Efficient online augmentation with range learning. *arXiv preprint*
203 *arXiv:2212.10553*, 2022.
- 204 [27] S. Mehta, S. Naderiparizi, F. Faghri, M. Horton, L. Chen, A. Farhadi, O. Tuzel, and M. Rastegari.
205 Rangeaugment: Efficient online augmentation with range learning, 2022.
- 206 [28] I. Misra, A. Shrivastava, A. Gupta, and M. Hebert. Cross-stitch networks for multi-task learning,
207 2016.
- 208 [29] P. K. Nathan Silberman, Derek Hoiem and R. Fergus. Indoor segmentation and support inference
209 from rgb-d images. In *ECCV*, 2012.
- 210 [30] X. Qi, R. Liao, Z. Liu, R. Urtasun, and J. Jia. Geonet: Geometric neural network for joint depth
211 and surface normal estimation. In *Proceedings of the IEEE Conference on Computer Vision*
212 *and Pattern Recognition*, pages 283–291, 2018.
- 213 [31] A. Radford, J. W. Kim, C. Hallacy, A. Ramesh, G. Goh, S. Agarwal, G. Sastry, A. Askell,
214 P. Mishkin, J. Clark, G. Krueger, and I. Sutskever. Learning transferable visual models from
215 natural language supervision. *CoRR*, abs/2103.00020, 2021. URL [https://arxiv.org/abs/](https://arxiv.org/abs/2103.00020)
216 [2103.00020](https://arxiv.org/abs/2103.00020).
- 217 [32] K. Ranasinghe, B. McKinzie, S. Ravi, Y. Yang, A. Toshev, and J. Shlens. Perceptual grouping
218 in contrastive vision-language models. *ICCV*, 2023.
- 219 [33] R. Ranftl, A. Bochkovskiy, and V. Koltun. Vision transformers for dense prediction. *CoRR*,
220 abs/2103.13413, 2021. URL <https://arxiv.org/abs/2103.13413>.
- 221 [34] S. Ruder. An overview of multi-task learning in deep neural networks. *arXiv preprint*
222 *arXiv:1706.05098*, 2017.
- 223 [35] O. Russakovsky, J. Deng, H. Su, J. Krause, S. Satheesh, S. Ma, Z. Huang, A. Karpathy,
224 A. Khosla, M. S. Bernstein, A. C. Berg, and L. Fei-Fei. Imagenet large scale visual recognition
225 challenge. *CoRR*, abs/1409.0575, 2014. URL <http://arxiv.org/abs/1409.0575>.
- 226 [36] C. Schuhmann, R. Beaumont, R. Vencu, C. Gordon, R. Wightman, M. Cherti, T. Coombes,
227 A. Katta, C. Mullis, M. Wortsman, et al. Laion-5b: An open large-scale dataset for training
228 next generation image-text models. *Advances in Neural Information Processing Systems*, 35:
229 25278–25294, 2022.
- 230 [37] M. Shukor, C. Dancette, A. Rame, and M. Cord. Unified model for image, video, audio and
231 language tasks, 2023.

- 232 [38] T. Sun, M. Segu, J. Postels, Y. Wang, L. Van Gool, B. Schiele, F. Tombari, and F. Yu. Shift:
233 a synthetic driving dataset for continuous multi-task domain adaptation. In *Proceedings of*
234 *the IEEE/CVF Conference on Computer Vision and Pattern Recognition*, pages 21371–21382,
235 2022.
- 236 [39] X. Sun, R. Panda, R. Feris, and K. Saenko. Adashare: Learning what to share for efficient deep
237 multi-task learning, 2020.
- 238 [40] T. Thrush, R. Jiang, M. Bartolo, A. Singh, A. Williams, D. Kiela, and C. Ross. Winoground:
239 Probing vision and language models for visio-linguistic compositionality. In *Proceedings of the*
240 *IEEE/CVF Conference on Computer Vision and Pattern Recognition*, pages 5238–5248, 2022.
- 241 [41] H. Touvron, T. Lavril, G. Izacard, X. Martinet, M.-A. Lachaux, T. Lacroix, B. Rozière, N. Goyal,
242 E. Hambro, F. Azhar, et al. Llama: Open and efficient foundation language models. *arXiv*
243 *preprint arXiv:2302.13971*, 2023.
- 244 [42] A. Vaswani, N. Shazeer, N. Parmar, J. Uszkoreit, L. Jones, A. N. Gomez, L. Kaiser, and
245 I. Polosukhin. Attention is all you need, 2023.
- 246 [43] P. Wang, A. Yang, R. Men, J. Lin, S. Bai, Z. Li, J. Ma, C. Zhou, J. Zhou, and H. Yang. Ofa:
247 Unifying architectures, tasks, and modalities through a simple sequence-to-sequence learning
248 framework, 2022.
- 249 [44] Z. Yang, Z. Gan, J. Wang, X. Hu, F. Ahmed, Z. Liu, Y. Lu, and L. Wang. Crossing the format
250 boundary of text and boxes: Towards unified vision-language modeling. *CoRR*, abs/2111.12085,
251 2021. URL <https://arxiv.org/abs/2111.12085>.
- 252 [45] P. Young, A. Lai, M. Hodosh, and J. Hockenmaier. From image descriptions to visual deno-
253 tations: New similarity metrics for semantic inference over event descriptions. *Transactions*
254 *of the Association for Computational Linguistics*, 2:67–78, 2014. doi: 10.1162/tacl_a_00166.
255 URL <https://aclanthology.org/Q14-1006>.
- 256 [46] J. Yu, Z. Wang, V. Vasudevan, L. Yeung, M. Seyedhosseini, and Y. Wu. Coca: Contrastive
257 captioners are image-text foundation models, 2022.
- 258 [47] H. Zhang, P. Zhang, X. Hu, Y.-C. Chen, L. H. Li, X. Dai, L. Wang, L. Yuan, J.-N. Hwang, and
259 J. Gao. Glipv2: Unifying localization and vision-language understanding, 2022.
- 260 [48] Y. Zhang, K. Gong, K. Zhang, H. Li, Y. Qiao, W. Ouyang, and X. Yue. Meta-transformer: A
261 unified framework for multimodal learning, 2023.
- 262 [49] H. Zhao, J. Shi, X. Qi, X. Wang, and J. Jia. Pyramid scene parsing network, 2017.

263 A Related Work

264 **Vision FMs.** Vision FMs extended the concept of pre-training to vast datasets containing hundreds
265 of millions or even billions of images. This was in part driven by the introduction of ViTs [8] which
266 demonstrated the scalability of training Transformers [42] to such large-scale datasets in the field of
267 computer vision. Since then, numerous large-scale pre-training methods have emerged in the domain
268 of computer vision [e.g., 31, 46, 3, 14]. Arguably, one of the most prominent classes of vision FMs is
269 CLIP that specializes in aligning noisy image-text pairs from the web [31, 36, 10]. This distinction is
270 not only attributed to its scalability, but also to its prompting capabilities and robustness in handling
271 dataset distribution shifts. Nevertheless, these models often face challenges in associating text with
272 individual objects and localizing them [40, 12, 32]. This work focuses on enhancing this capability
273 through pseudo-supervision.

274 **Pseudo-supervision with experts.** The primary objective of pseudo-supervision [19] is to facilitate
275 model training by generating pseudo-labels for unlabeled data, typically leveraging experts trained
276 on a subset of the data containing ground truth labels. This methodology has also been applied to the
277 training of foundation models (FMs). To the best of our knowledge, current approaches involve the
278 acquisition of crowd labels for a portion of the data on a *single* task, with the subsequent training of
279 experts on this labeled subset [e.g., 11, 47, 16, 24]. These trained experts are then utilized to create
280 pseudo-labels for the remaining unlabeled data. Essentially, these methods employ experts that have
281 been trained on the same or similar data distribution as the unlabeled data, aiming to achieve positive
282 transfer. For example, in GLIP [20], a subset of web data is crowd-sourced to obtain localization
283 labels, which is then used for expert training. Following expert training, these experts are employed to
284 generate pseudo-labels for the remaining unlabeled web data. This combination of crowd labels and
285 pseudo-labels is subsequently used to train the GLIP V2 [47] model. SAM [16] also follows similar
286 paradigm for creating large-scale segmentation dataset. Unlike previous approaches, our proposed
287 method uses publicly accessible experts trained on diverse tasks with different data distributions and
288 objectives.

289 **Multi-task learning for FMs.** Multi-tasking [4, 34], a standard method for training on multiple
290 tasks simultaneously, is widely used in machine learning [23, 28, 39], including FMs [e.g., 43, 5,
291 44, 37, 48]. Existing multi-task FMs creates a unified multi-task datasets by either collecting a new
292 labeled dataset [e.g., 38] or mixing existing labeled datasets [e.g., 25], to facilitate positive transfer of
293 knowledge to down-stream tasks. In contrast, CLIPTeX does not need any data collection and uses
294 pseudo-supervision for training.

295 A.1 Positive Transfer of Representations from CLIPTeX to Downstream Tasks

296 The CC3M dataset is uncurated and noisy, and may have a skewed distribution towards specific
297 object classes or scenes. Consequently, knowledge transfer from experts to CLIPTeX may also be
298 skewed towards more frequent objects in the data. To explore this phenomenon, we quantified the
299 frequency of objects (bounding boxes or instances) in the pseudo-labels generated by the Mask
300 R-CNN expert (Fig. 2a) on the CC3M dataset. Additionally, we examined class-wise improvements
301 in IoU of CLIPTeX with respect to CLIP-FT on the PASCAL VOC dataset (Fig. 2b). CLIPTeX
302 improves the IoU for all classes in the PASCAL VOC dataset and is not biased towards the most
303 frequently occurring object classes. These findings, combined with insights in Section 4 suggests
304 positive transfer of representations from CLIPTeX to down-stream tasks.

305 B Task-head complexity

306 As discussed in Section 2, we use light-weight heads to improve visual representations in CLIP’s
307 image encoder. We replace these heads with heavier counterparts (comprising of three standard
308 convolutional layers) when training CLIPTeX with CC3M pseudo-labels. Table 4 shows that light-
309 weight heads deliver similar performance to heavy-weight heads in most cases. Therefore, we use
310 light-weight heads for pseudo-supervision in our experiments to make the training more efficient.

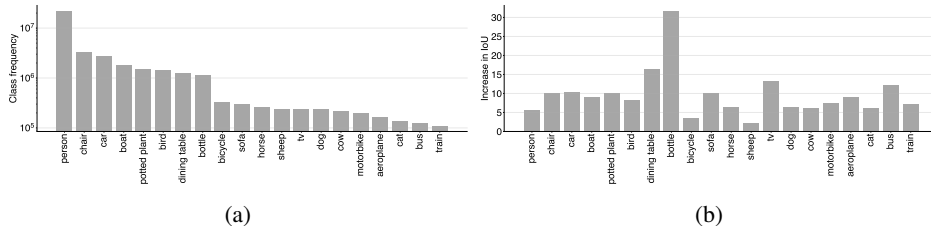


Figure 2: **Positive transfer with CLIPTeX**. (a) Bounding box frequency for PASCAL VOC classes in CC3M’s pseudo-labels obtained with Mask R-CNN. (b) Class-wise IoU gap (in %) between CLIP-FT and CLIPTeX when linear probed on the PASCAL VOC.

Table 4: **Role of head complexity (light and heavy) when training with pseudo-labels on CC3m**. #layers denote the number of convolutional layers used in the task head. Results with different probes for different dense prediction tasks are reported (see Section 3 for details). For segmentation, we report the results on the PASCAL VOC dataset. We observe similar trends in ADE20k dataset.

# layers	Segmentation (\uparrow)		Detection (\uparrow)		Depth (\downarrow)		Surface Normal (\uparrow)	
	Linear	PSPNet	Mask R-CNN	SSD	Linear	PSPNet	Linear	PSPNet
1	73.43	80.71	28.89	17.50	0.159	0.128	39.96	50.80
3	66.70	80.24	28.64	17.43	0.155	0.127	40.55	51.72

311 C Results

312 Tables 5 to 7 compares the results of CLIPTeX with other baselines on different tasks and datasets with
 313 different heads. We observe that pseudo-supervision via experts in CLIPTeX improves performance
 314 by large across different tasks and datasets.

Table 5: **Probing results for semantic segmentation**. A higher value of mIoU is better.

Model	ADE20k			PascalVOC		
	Linear	DeepLabV3	PSPNet	Linear	DeepLabV3	PSPNet
ViT-B/16						
CLIP	6.78	16.15	17.32	18.66	43.75	45.53
CLIP-FT	26.60	37.11	38.80	62.47	77.67	78.22
CLIPTeX (Ours)	29.26	39.20	39.70	73.43	80.57	80.71
ViT-H/16						
CLIP	24.18	33.39	34.86	56.18	73.12	75.37
CLIP-FT	32.20	43.05	44.24	62.95	81.73	82.94
CLIPTeX (Ours)	36.17	45.43	45.63	79.30	84.06	84.31
ResNet-50						
CLIP	11.98	29.51	28.22	46.96	70.34	70.92
CLIP-FT	11.30	34.86	33.97	34.78	73.70	74.17
CLIPTeX (Ours)	12.93	35.45	34.80	40.31	75.82	75.58

315 D Hyperparameters

316 Hyper-parameters used during training and probing CLIPTeX and other models are given in Table 8
 317 and Table 9 respectively.

Table 6: **Probing results for object detection, instance segmentation, and image classification.** In (a), for Mask R-CNN, we report mAP (higher is better) for bounding box and instance segmentation while for SSD, we report mAP only for bounding box on the COCO dataset. In (b) top-1 accuracy (higher is better) is reported.

(a) Detection and instance segmentation on COCO.				(b) Image classification.		
Model	Mask R-CNN		SSD	Model	ImageNet	Places365
	BBox	Instance	BBox			
ViT-B/16				ViT-B/16		
CLIP	15.20	12.16	5.33	CLIP	80.24	55.52
CLIP-FT	27.21	23.18	16.46	CLIP-FT	79.94	55.21
CLIPTeX (Ours)	28.89	24.92	17.50	CLIPTeX (Ours)	79.64	55.36
ViT-H/16				ViT-H/16		
CLIP	26.65	21.29	11.07	CLIP	84.85	56.96
CLIP-FT	33.93	28.92	20.24	CLIP-FT	84.1	55.81
CLIPTeX (Ours)	34.50	29.60	21.55	CLIPTeX (Ours)	83.2	55.96
ResNet-50				ResNet-50		
CLIP	29.49	25.61	20.32	CLIP	78.35	56.55
CLIP-FT	38.13	34.02	30.28	CLIP-FT	78.92	56.98
CLIPTeX (Ours)	38.23	34.04	28.62	CLIPTeX (Ours)	78.95	57.22

Table 7: **Probing results for depth and surface normal estimation on NYU-V2 dataset.** Following Lasinger et al. [18], we report absolute relative error (lower is better) for depth estimation. For surface normal estimation, we report $a < 30$ following Bae et al. [1] (higher is better).

(a) Depth estimation.				(b) Surface normal estimation.			
Model	Linear	DeepLabV3	PSPNet	Model	Linear	DeepLabV3	PSPNet
ViT-B/16				ViT-B/16			
CLIP	0.235	0.189	0.168	CLIP	28.49	45.17	47.29
CLIP-FT	0.215	0.145	0.139	CLIP-FT	29.06	47.74	47.91
CLIPTeX (Ours)	0.159	0.129	0.128	CLIPTeX (Ours)	39.96	50.95	50.80
ViT-H/16				ViT-H/16			
CLIP	0.212	0.151	0.132	CLIP	29.09	47.31	49.78
CLIP-FT	0.213	0.131	0.125	CLIP-FT	29.21	49.73	50.48
CLIPTeX (Ours)	0.138	0.118	0.117	CLIPTeX (Ours)	43.22	53.23	53.89
ResNet-50				ResNet-50			
CLIP	0.212	0.156	0.147	CLIP	33.67	46.05	47.28
CLIP-FT	0.239	0.160	0.155	CLIP-FT	28.72	46.99	48.66
CLIPTeX (Ours)	0.220	0.153	0.150	CLIPTeX (Ours)	31.56	47.92	49.44

Table 8: **Hyper-parameters for training CLIPTeX on CC3M dataset..**

Hyper-parameter	Value
Epochs	30
LR scheduler	cosine
Warmup Steps	1000
Warmup Init LR	1e-06
Maximum LR	3e-05
Minimum LR	1e-06
Batch size	32
λ_{depth}	1.0
λ_{clip}	1.0
λ_{seg}	0.1
$\lambda_{\text{surface normal}}$	1.0

Table 9: Hyper-parameters used for probing on different downstream tasks.

Hyper-parameter	Segmentation			Detection		Depth			Surface Normal			Classification
	Linear	DeepLabv3	PSPNet	Mask R-CNN	SSD	Linear	DeepLabv3	PSPNet	Linear	DeepLabv3	PSPNet	Linear
Epochs	50	50	50	25	200	50	50	50	50	50	50	40
LR scheduler	cosine	cosine	cosine	multi-step	cosine	cosine	cosine	cosine	cosine	cosine	cosine	cosine
Warmup Steps	500	500	500	250	500	1000	1000	1000	1000	1000	1000	1000
Warmup Init LR	1e-06	1e-06	1e-06	1e-05	9e-05	1e-06	1e-06	1e-06	1e-06	1e-06	1e-06	1e-06
Maximum LR	3e-05	3e-05	3e-05	3e-04	9e-04	1e-04	1e-04	1e-04	1e-05	1e-05	1e-05	3e-05
Minimum LR	3e-06	3e-06	3e-06	NA	1e-06	1e-06	1e-06	1e-06	1e-06	1e-06	1e-06	1e-06
LR Milestones	NA	NA	NA	[22, 24]	NA	NA	NA	NA	NA	NA	NA	NA
LR Gamma	NA	NA	NA	0.1	NA	NA	NA	NA	NA	NA	NA	NA
Batch size	32	32	32	4	32	16	16	16	16	16	16	128